2007 IEEE International Conference on
Robotics and Automation
Roma, Italy, 10-14 April 2007

Blind Grasp and Manipulation of a Rigid Object by a Pair of Robot Fingers with Soft Tips

Morio Yoshida, Suguru Arimoto, and Ji-Hun Bae

Abstract— **This paper is concerned with construction of a mathematical model for a class of lumped-parameter dynamics of a pair of robot fingers with soft and deformable tips pinching a rigid object. It is then shown that, in the case of a pair of planer fingers with two and three joints and a 2-D rigid object with parallel or non-parallel flat surfaces, there exists a sensory-motor coordinated control signal constructed by using only the knowledge of finger kinematics and measurements of finger joints such that it realizes secure grasping in a dynamic sense. This shows that a pair of robot fingers can grasp a thing securely in a blind manner. The result is further extended to the case of 3-D object grasping and manipulation by a pair of soft fingers, one of which can move in 3-D space.**

I. Introduction

It is the hand that is most intriguing and most human of appendages. This motivated many prominent roboticists to design and make sophisticated multi-fingered robotic mechanisms imitating the human hand (see the literature[1] $\sim$ [5]). However, of so many research works on robotic hands there is a dearth of papers that explored a key function of the human hand called "precision prehension" based upon "finger-thumb opposition". Indeed, opposability of the thumb against the index finger or other digits is a key characteristics that distinguishes the humankind from primates, as well as bipedal walking and tool-making (see[6]).

This paper attempts to explore physical and mechanical meanings of the prehensility of a pair of multi-joint robot fingers with soft and deformable tips in both cases of 2D and 3D object grasps and manipulations. In this paper, "prehensility" is defined as the ability to grasp an object and hold it securely in one hand[6]. Hence, the purpose of this paper is to show that the prehensility can be functioned in a mechanical setup of dual multi-joint fingers with soft tips through implementing a sensory-motor coordinated control signal.

Stable grasp by means of a pair of robot fingers with soft tips was first investigated by Montana [7], but stability of a grasp or prehensility is treated in a semi-dynamic meaning. Arimoto et al. [8] $\sim$ [11] found an important role of rolling constraint forces arising in tangential directions to the object surfaces. However, their stability analysis was not mathematically rigorous, though it was based upon Lagrange' equation of motion of the overall fingers-object system. In recent years, rigorous analysis of stable grasp in the sense of prehensibility has been presented in the case of rigid contacts when finger-tips are rigid and hemi-spherical, owing to finding of a class of control signals constructed by only using finger kinematics and measurement of fingers joint angles without use of any object kinematics, location of its mass center, or external visual or tactile sensing [11] $\sim$ [13]. Hence, Arimoto et al. [11] $\sim$ [13] called such a prehensility by means of a pair of robot fingers "blind grasping".

This paper extends those results obtained in the case of rigid contacts to the case of robot fingers equipped with soft and deformable tips. The most crucial difference of prehensility between the rigid contact case and the soft area contact one is that in the former a stability region of grasp of a thin and light object becomes narrow in its margin but in the latter any thinner objects with flat surfaces can be grasped securely with a larger stability margin.

Secondly, motivated from the previous results concerning "blind grasping" in the case of rigid finger-ends (see [7]), a class of control signals is proposed, which can be constructed easily by using only physical parameters of fingers and measurement data on finger joints. It is shown theoretically that such a control signal renders the closed-loop dynamics asymptotically stable on an equilibrium manifold toward satisfying force/torque balance in a dynamic sense. This shows that a pair of robot fingers can grasp a thing securely in a blind manner, that is, without knowing object kinematics or using external sensings such as tactile or visual sensing. Numerical simulation results are also given to verify the theoretical predictions.

II. Dynamics of PINCHING

Firstly let us derive dynamics of pinch motion by a pair of two and three DOF (Degrees-of-Freedom) fingers with soft tips (see Fig. 1). In this setup, symbols O and O$'$ denote first joint centers of the left and right fingers respectively, point O also denotes the origin of Cartesian coordinates fixed at the base frame, and $\mathrm{O}_{\mathrm{c.m.}}$ denotes the center of mass of the object whose position is expressed in terms of $\boldsymbol{x} = (x, y)^{\mathrm{T}}$ of the Cartesian coordinates. Symbols O_1 and O_2 denote centers of area contacts whose Cartesian coordinates are described as $\boldsymbol{x}_1 = (x_1, y_1)^{\mathrm{T}}$ and $\boldsymbol{x}_2 = (x_2, y_2)^{\mathrm{T}}$ respectively and O_{01} and O_{02} denote centers of hemispherical soft finger tips which are expressed in terms of Cartesian coordinates as $\boldsymbol{x}_{0i} = (x_{0i}, y_{0i})^{\mathrm{T}}$,(i=1,2) respectively. Next let us denote

M. Yoshida and S. Arimoto are with the Bio-Mimetic Control Research Center, RIKEN, 2271-130, Anagahora, Shimoshidami, Moriyama-ku, Nagoya, Aichi, 463-0003, Japan

S. Arimoto is with the Department of Robotics, Ritsumeikan University,1-1-1 Nojihigashi Kusatu city 525-8577, Japan arimoto@se.ritsumei.ac.jp

Ji-Hun Bae is with Pohang Institute of Intelligent Robotics, San 31, Hyoja-Dong, Nam-Gu, Pohang, Gyeongbuk 790-784, S.Korea joseph@postech.ac.kr

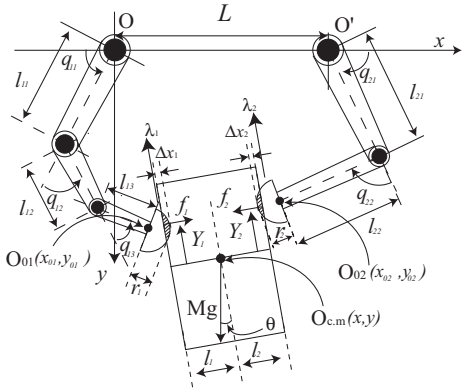

Fig. 1. Two robot fingers pinching an object with parallel flat surfaces under the gravity effect

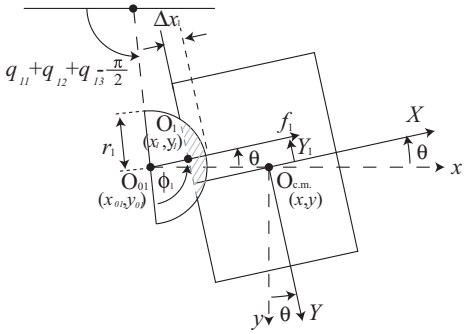

Fig. 2. Definition of physical variables

the Y-component of center O_1 of area-contact of the left finger in terms of Cartesian coordinates (X, Y) fixed at the object (see Figs.1 and 2) by Y_1 and that of the right finger by Y_2. Other symbols L, l_i, and l_{ij} are defined in Fig.1. Then, obviously it follows that

$$\Delta x_i = r_i + l_i + (-1)^i (\boldsymbol{x} - \boldsymbol{x}_{0i})^{\mathrm{T}} \boldsymbol{r}_X \quad (1)$$

$$\boldsymbol{x}_i = \boldsymbol{x}_{0i} - (-1)^i (r_i - \Delta x_i) \boldsymbol{r}_X \quad (2)$$

where $\Delta x_i (i = 1, 2)$ denote the maximum displacements of deformation arised in centers of area-contact respectively and $\boldsymbol{r}_X = (\cos\theta, -\sin\theta)^{\mathrm{T}}$. Similarly, it follows that

$$\boldsymbol{x} = \boldsymbol{x}_1 + l_1 \boldsymbol{r}_X - Y_1 \boldsymbol{r}_Y = \boldsymbol{x}_2 - l_2 \boldsymbol{r}_X - Y_2 \boldsymbol{r}_Y \quad (3)$$

from which it follows that

$$Y_i = (\boldsymbol{x}_{0i} - \boldsymbol{x})^{\mathrm{T}} \boldsymbol{r}_Y, \qquad i = 1, 2 \quad (4)$$

where $\boldsymbol{r}_Y = (\sin\theta, \cos\theta)^{\mathrm{T}}$. Since velocities of O_1 (the center of the left hand contact area, see Fig.2) in terms of finger-end coordinates and in terms of object coordinates $\mathrm{O}_{\mathrm{c.m.}} - XY$ are equal, it follows that

$$-(r_1 - \Delta x_1) \frac{\mathrm{d}}{\mathrm{d}t} \left(\frac{3\pi}{2} + \theta - \boldsymbol{q}_1^{\mathrm{T}} \boldsymbol{e}_1 \right) = \frac{\mathrm{d}}{\mathrm{d}t} Y_1 \quad (5)$$

where $\boldsymbol{e}_1 = (1, 1, 1)^{\mathrm{T}}$. Similarly, it follows that

$$-(r_2 - \Delta x_2) \frac{\mathrm{d}}{\mathrm{d}t} \left(\frac{3\pi}{2} - \theta - \boldsymbol{q}_2^{\mathrm{T}} \boldsymbol{e}_2 \right) = \frac{\mathrm{d}}{\mathrm{d}t} Y_2 \quad (6)$$

where $\boldsymbol{e}_2 = (1, 1)^{\mathrm{T}}$. Equations (5) and (6) are of the form of total differentials. Hence, it is reasonable to introduce Lagrange multiplies λ_i in such a way that

$$0 = \lambda_i \left\{ \frac{\mathrm{d}Y_i}{\mathrm{d}t} + (r_i - \Delta x_i) \frac{\mathrm{d}}{\mathrm{d}t} \left(\frac{3}{2}\pi - (-1)^i \theta - \boldsymbol{q}_i^{\mathrm{T}} \boldsymbol{e}_i \right) \right\} \quad (7)$$

$$i = 1, 2 \quad (8)$$

According to the lumped-parametrization of contact forces caused by defomation of finger-tip material (see Appendix A of paper [8]), the reproducing force $\bar{f}_i(\Delta x_i)$ arizing in the direction normal to the object surfaces at the center $\mathrm{O_i}$ of contact area is characterized as

$$\bar{f}_i(\Delta x_i) = k_i \Delta x_i^2, \quad i = 1, 2 \quad (9)$$

with stiffness parameter $k_i{>}0[\mathrm{N/m^2}]$. Furthermore, we assume that lumped parametrized viscous forces also arise from distributed viscosity of the finger-tip material, which are accompanied with reproducing forces in such a way that

$$f_i(\Delta x_i, \Delta \dot{x}_i) = \bar{f}_i(\Delta x_i) + \xi_i(\Delta x_i) \Delta \dot{x}_i \quad (10)$$

where $\xi_i(\Delta x_i)$ is a positive scalar function increasing with increase of Δx_i. Then the total potential energy of reproducing forces and the total kinetic energy can be given as

$$P = P_1 + P_2 - Mgy + \sum_{i=1}^{2} \int_0^{\Delta x_i} \bar{f}_i(\xi) \mathrm{d}\xi \quad (11)$$

$$K = \frac{1}{2} \left\{ \sum_{i=1,2} \dot{\boldsymbol{q}}_i^{\mathrm{T}} H_i(\boldsymbol{q}_i) \dot{\boldsymbol{q}}_i + M \parallel \dot{\boldsymbol{x}} \parallel^2 + I\dot{\theta}^2 \right\} \quad (12)$$

where $H_i (i = 1, 2)$ and I denote inertia moments of the fingers $i = 1, 2$ and the object respectively, M denotes the mass of the object, P_i the potential energy for finger i, and $-Mgy$ denotes that of the object. Finally, the Lagrange equation of motion of the overall system can be derived by applying Hamilton's principle described as

$$\int_{t_0}^{t_1} \Bigg[\delta(K - P) - \sum_{i=1,2} \frac{\partial \frac{1}{2} \left\{ \xi_i(\Delta x_i) \Delta \dot{x}_i^2 \right\}}{\partial \Delta \dot{x}_i} \delta \Delta x_i + \sum_{i=1,2} \lambda_i \left\{ \frac{\partial Y_i}{\partial \boldsymbol{z}} + (r_i - \Delta x_i) \frac{\partial \phi_i}{\partial \boldsymbol{z}} \right\}^{\mathrm{T}} \delta \boldsymbol{z} + \sum_{i=1,2} \boldsymbol{u}_i^{\mathrm{T}} \delta \boldsymbol{q}_i \Bigg] \mathrm{d}t = 0 \quad (13)$$

where $\boldsymbol{z} = (\boldsymbol{q}_1^{\mathrm{T}}, \boldsymbol{q}_2^{\mathrm{T}}, x, y, \theta)^{\mathrm{T}}$ and $\phi_i = -(-1)^i \theta - \boldsymbol{q}_i^{\mathrm{T}} \boldsymbol{e}_i$, which results in

$$H_i(\boldsymbol{q}_i) \ddot{\boldsymbol{q}}_i + \left(\frac{1}{2} \dot{H}_i + S_i \right) \dot{\boldsymbol{q}}_i - (-1)^i f_i J_{0i}^{\mathrm{T}} \boldsymbol{r}_X + \lambda_i \left\{ (r_i - \Delta x_i) \boldsymbol{e}_i - J_{0i}^{\mathrm{T}} \boldsymbol{r}_Y \right\} + g_i(\boldsymbol{q}_i) = \boldsymbol{u}_i \quad (14)$$

$$M\ddot{\boldsymbol{x}} - (\boldsymbol{r}_X, \boldsymbol{r}_Y)(f_1 - f_2, -\lambda_1 - \lambda_2)^{\mathrm{T}} - (0, Mg)^{\mathrm{T}} = \boldsymbol{0} \quad (15)$$

$$I\ddot{\theta} - f_1 Y_1 + f_2 Y_2 + l_1 \lambda_1 - l_2 \lambda_2 = 0 \quad (16)$$

where $J_{0i}^{\mathrm{T}} = \partial \boldsymbol{x}_{0i}^{\mathrm{T}} / \partial \boldsymbol{q}_i$ and S_i is a skew-symmetric matrix (see [14]). It is obvious that the input-ouput pair

$\boldsymbol{u}=(\boldsymbol{u}_1,\boldsymbol{u}_2)^{\mathrm{T}}, \dot{\boldsymbol{q}}=(\dot{\boldsymbol{q}}_1,\dot{\boldsymbol{q}}_2)^{\mathrm{T}}$ concerning the dynamics of eqs.(13) to (15) satisfies the equation

$$\int_0^t \left(\dot{\boldsymbol{q}}_1^{\mathrm{T}}\boldsymbol{u}_1+\dot{\boldsymbol{q}}_2^{\mathrm{T}}\boldsymbol{u}_2\right)\mathrm{d}\tau = E(t)-E(0) - \int_0^t \sum_{i=1,2} \xi\left(\Delta x_i(\tau)\right)\Delta\dot{x}_i^2(\tau)\mathrm{d}\tau \tag{17}$$

where $E=K+P$.

III. Control signals for Blind Grasping

Motivated from the analysis in the case of rigid rolling contacts between rigid finger-ends and a rigid object (see [12]), we propose the following control signal that should exert torques on finger joints:

$$\boldsymbol{u}_i = g_i(\boldsymbol{q}_i) - c_i\dot{\boldsymbol{q}}_i + (-1)^i\frac{f_d}{r_1+r_2}\boldsymbol{J}_{0i}^{\mathrm{T}}\begin{pmatrix} x_{01}-x_{02} \\ y_{01}-y_{02}\end{pmatrix} - \frac{\hat{M}g}{2}\left(\frac{\partial y_{0i}}{\partial \boldsymbol{q}_i}\right) - r_i\hat{N}_i\boldsymbol{e}_i \quad i=1,2 \tag{18}$$

where

$$\hat{M} = \hat{M}(0) + \int_0^t \frac{g\gamma_M^{-1}}{2}\sum_{i=1,2}\left(\frac{\partial y_{0i}}{\partial \boldsymbol{q}_i}\right)^{\mathrm{T}}\dot{\boldsymbol{q}}_i\,\mathrm{d}\tau = \hat{M}(0) + \frac{g\gamma_M^{-1}}{2}\left(y_{01}(t)+y_{02}(t) - y_{01}(0)-y_{02}(0)\right) \tag{19}$$

$$\hat{N}_i = \gamma_{N_i}^{-1}\int_0^t \left(r_i\boldsymbol{e}_i^{\mathrm{T}}\dot{\boldsymbol{q}}_i\right)\mathrm{d}\tau = \gamma_{N_i}^{-1}r_i\boldsymbol{e}_i^{\mathrm{T}}\left(\boldsymbol{q}_i(t)-\boldsymbol{q}_i(0)\right)\ (i=1,2) \tag{20}$$

and γ_M and $\gamma_{Ni}(i=1,2)$ are positive constants. In this form, nothing differes from that of control signal proposed in the rigid contact case. The third term of the right hand side of eq.(18) is a signal based upon the opposable force between O_{01} and O_{02} (not between O_1 and O_2, because positions of O_1 and O_2 can not be measured). The fourth term stands for compensation for the object mass based upon its estimator. The fifth term is introduced for saving excess movements of finger joints from the initial pose.

IV. Theoretical Proof of Feasibility of Blind Grasping

First, define

$$\begin{cases} \Delta f_i = f_i + (-1)^i\frac{Mg}{2}\sin\theta + \frac{f_d}{r_1+r_2}\left(\boldsymbol{x}_{01}-\boldsymbol{x}_{02}\right)^{\mathrm{T}}\boldsymbol{r}_X \\ \Delta\lambda_i = \lambda_i - \frac{Mg}{2}\cos\theta + (-1)^i\frac{f_d}{r_1+r_2}\left(\boldsymbol{x}_{01}-\boldsymbol{x}_{02}\right)^{\mathrm{T}}\boldsymbol{r}_Y \\ N_i = (-1)^i\frac{f_d}{r_1+r_2}\left(\boldsymbol{x}_{01}-\boldsymbol{x}_{02}\right)^{\mathrm{T}}\boldsymbol{r}_Y - \frac{Mg}{2}\cos\theta \end{cases} \tag{21}$$

$$\begin{cases} S = -f_d\left(1-\frac{\Delta x_1+\Delta x_2}{r_1+r_2}\right)(Y_1-Y_2) - \frac{Mg}{2}N \\ N = (Y_1+Y_2)\sin\theta - (l_1-l_2)\cos\theta \end{cases} \tag{22}$$

Note that from eq.(4) and eq.(1)

$$\begin{cases} \left(\boldsymbol{x}_{01}-\boldsymbol{x}_{02}\right)^{\mathrm{T}}\boldsymbol{r}_Y = Y_1-Y_2 \\ -\left(\boldsymbol{x}_{01}-\boldsymbol{x}_{02}\right)^{\mathrm{T}}\boldsymbol{r}_X = l_1+l_2+r_1+r_2-(\Delta x_1+\Delta x_2) \end{cases} \tag{23}$$

Next define

$$f_0 = f_d\left\{1+\frac{l_1+l_2-\Delta x_1-\Delta x_2}{r_1+r_2}\right\} \tag{24}$$

Differently from the case of rigid finger-ends [12], f_0 is not a constant but dependent on the magnitude of $\Delta x_1+\Delta x_2$. Nevertheless, it is possible to find $\Delta x_{di}(i=1,2)$ for a given $f_d>0$ so that they satisfy

$$\begin{cases} \bar{f}_1(\Delta x_{d1}) = \left(1+\frac{l_1+l_2-\Delta x_{d1}-\Delta x_{d2}}{r_1+r_2}\right)f_d \\ \bar{f}_2(\Delta x_{d2}) = \left(1+\frac{l_1+l_2-\Delta x_{d1}-\Delta x_{d2}}{r_1+r_2}\right)f_d \end{cases} \tag{25}$$

because $\bar{f}_i(\Delta x)$ is of the form of $\bar{f}_i(\Delta x)=k_i\Delta x^2$ [8]. Then, by substituting eq.(17) into eq.(13) and referring to eqs.(20) to (22), we obtain the closed-loop dynamics of the overall fingers-object system in the following way:

$$H_i(\boldsymbol{q}_i)\ddot{\boldsymbol{q}}_i + \left(\frac{1}{2}\dot{H}_i+S_i\right)\dot{\boldsymbol{q}}_i - (-1)^i\Delta f_i J_{0i}^{\mathrm{T}}\boldsymbol{r}_X - \Delta\lambda_i\boldsymbol{r}_{\lambda i} - \Delta Mg\frac{\partial y_{0i}}{\partial \boldsymbol{q}_i} - r_i\Delta N_i\boldsymbol{e}_i = 0 \tag{26}$$

$$M\ddot{\boldsymbol{x}} - (\Delta f_1-\Delta f_2)\boldsymbol{r}_X - (\Delta\lambda_1+\Delta\lambda_2)\boldsymbol{r}_Y = 0 \tag{27}$$

$$I\ddot{\theta} - \Delta f_1 Y_1 + \Delta f_2 Y_2 + l_1\Delta\lambda_1 - l_2\Delta\lambda_2 + S = 0 \tag{28}$$

where $\Delta N_i = \hat{N}_i - (1-\Delta x_i/r_i)N_i(i=1,2)$ and

$$\boldsymbol{r}_{\lambda i} = -\left\{(r_i-\Delta x_i)\boldsymbol{e}_i - J_{0i}^{\mathrm{T}}\boldsymbol{r}_Y\right\} \tag{29}$$

Then, it is important to note that along a solution to the equations of (26) to (28) under the constraints of eqs.(5) & (6) the following energy relation is satisfied:

$$\frac{\mathrm{d}}{\mathrm{d}t}W = \sum_{i=1,2} -\left\{c_i\|\dot{\boldsymbol{q}}_i\|^2 + \xi(\Delta x_i)\Delta\dot{x}_i^2\right\} \tag{30}$$

where

$$W = K+\Delta P + \frac{f_d}{2(r_1+r_2)}(Y_1-Y_2)^2 + \frac{\gamma_M}{2}\Delta M^2 + \sum_{i=1,2}\frac{\gamma_{Ni}}{2}\hat{N}_i^2 + \frac{Mg}{2}\left\{(y_{01}+y_{02}-2y)\right\} \tag{31}$$

$$\frac{y_{01}+y_{02}}{2} - y = \frac{Y_1+Y_2}{2}\cos\theta - \frac{1}{2}\left\{(l_1-l_2) + (r_1-r_2) - (\Delta x_1-\Delta x_2)\right\}\sin\theta \tag{32}$$

$$\Delta P = \sum_{i=1,2}\int_0^{\delta x_i}\left\{\bar{f}_i(\Delta x_{di}+\xi) - \bar{f}_i(\Delta x_{di})\right\}\mathrm{d}\xi \tag{33}$$

where $\delta x_i = \Delta x_i - \Delta x_{di}$. Now, it is convenient to define

$$\Delta\boldsymbol{\lambda} = \left(\Delta\bar{f}_1,\Delta\bar{f}_2,\Delta\lambda_1,\Delta\lambda_2,\frac{\Delta M}{2}g,\Delta N_1,\Delta N_2,\frac{S}{r_3}\right)^{\mathrm{T}} \tag{34}$$

$$A=\begin{bmatrix} -J_1^{\mathrm{T}}\boldsymbol{r}_X & 0 & \boldsymbol{r}_{\lambda 1} & 0 \\ 0 & J_2^{\mathrm{T}}\boldsymbol{r}_X & 0 & \boldsymbol{r}_{\lambda 2} \\ r\cos\theta & -r\cos\theta & -r\sin\theta & -r\sin\theta \\ -r\sin\theta & r\sin\theta & -r\cos\theta & -r\cos\theta \\ Y_1 & -Y_2 & -l_1 & l_2 \end{bmatrix} \tag{35}$$

$$D=\begin{bmatrix} -\frac{\partial y_{01}}{\partial \boldsymbol{q}_1} & -r_1\boldsymbol{e}_1 & 0 & 0 \\ -\frac{\partial y_{02}}{\partial \boldsymbol{q}_2} & 0 & -r_2\boldsymbol{e}_2 & 0 \\ 0 & 0 & 0 & 0 \\ 0 & 0 & 0 & 0 \\ 0 & 0 & 0 & r_3 \end{bmatrix} \tag{36}$$

where $\Delta\bar{f}_i = \Delta f_i - \xi_i(\Delta x_i)\Delta\dot{x}_i$. Then, the closed-loop dynamics of (26), (27), and (28) can be expressed in the following unified matrix-vector form:

$$H\ddot{\bar{\boldsymbol{z}}} + \left(\frac{1}{2}\dot{H} + S\right)\dot{\bar{\boldsymbol{z}}} + C\dot{\bar{\boldsymbol{z}}} - [A, D]\Delta\boldsymbol{\lambda} + \sum_{i=1,2}\xi(\Delta x_i)\Delta\dot{x}_i\left(\frac{\partial\Delta x_i}{\partial\bar{\boldsymbol{z}}}\right) = 0 \tag{37}$$

where $\bar{\boldsymbol{z}} = \left(\boldsymbol{q}_1^{\mathrm{T}}, \boldsymbol{q}_2^{\mathrm{T}}, r^{-1}\boldsymbol{x}^{\mathrm{T}}, \theta\right)^{\mathrm{T}}$,

$$\begin{cases} H = \mathrm{diag}(H_1, H_2, r^2MI_2, I) \\ S = \mathrm{diag}(S_1, S_2, 0, 0, 0) \\ C = \mathrm{diag}(c_1I_3, c_2I_2, 0, 0, 0) \end{cases} \tag{38}$$

a positive scale factor r is introduced to balance numerical values of coefficients among motion equations in terms of $\dot{\boldsymbol{x}}$ with the physical unit of force [N] and rotational motion equations of $\dot{\boldsymbol{q}}_i$ and $\dot{\theta}$ with the unit of torque [Nm], and $r_3 > 0$ is also an appropriate scale factor. Next, define

$$p_1 = \sum_{j=1}^{3} q_{1j}, \quad p_2 = \sum_{j=1}^{2} q_{2j} \tag{39}$$

and note that $(Y_1 - Y_2)^2$ is quadratic in $x_{01} - x_{02}$ and $y_{01} - y_{02}$ and $\hat{N}_i^2$ for i=1, 2 are quadratic in p_1 and p_2. It follows from the definition of ΔP that ΔP is a positive definite function in δx_1 and δx_2. Hence, it is easy to check that W has a minimum W_m under the constraints of eqs.(5) & (6). This means that $\|\dot{\bar{\boldsymbol{z}}}\|$ is bounded and thereby it is possible to show that $\|\Delta\boldsymbol{\lambda}\|$ is bounded from eq.(37) and constraints of eqs.(5) & (6). Thus, $\ddot{\bar{\boldsymbol{z}}}$ becomes bounded and thereby $\dot{\bar{\boldsymbol{z}}}$ becomes uniformly continuous in t. Since $\dot{\boldsymbol{q}}_i(t)(i = 1, 2)$ and $\Delta\dot{x}_i$ are in $L^2(0, \infty)$ from (30), it follows from the well-know lemma (see Appendix C of [14]) that $\dot{\boldsymbol{q}}_i(t) \to 0$ and $\Delta\dot{x}_i(t) \to 0$ as $t \to \infty$, which means that $\dot{\theta}(t) \to 0$ as $t \to \infty$ from constraints of eqs.(5) & (6). Since the matrix $[A, D]$ is of an 8×8 squared matrix and nonsingular as easily checked, it follows that $\Delta\boldsymbol{\lambda}(t) \to 0$ as $t \to \infty$. Thus, as $t \to \infty$ the force/torque balance is established in a dynamic sense.

The proof presented above has been rather sketchy owing to limitation of given pages, but it can be ascertained by carrying out numerical simulations.

Further, it should be remarked that dynamics of the overall fingers-object system depicted in Fig.1 is redundant in degrees-of-freedom. In fact, the dimension of the generalized position coordinates is eight and there are two holonomic constraints concerning rolling. Therefore, the total d.o.f of the overall system is six. Then, the force/torque balance is realized through specification of physical values of Δx_1, Δx_2, λ_1, λ_2, and the magnitude of $y - (y_{01} + y_{02})/2$. Thus, one d.o.f is redundant. Actually, blind grasping can be realized when each robot finger has the two d.o.f, though in this case $\Delta\boldsymbol{\lambda}(t)$ in (37) converges to some non-zero constant vector $\Delta\boldsymbol{\lambda}_\infty$ as $t \to \infty$. The details of the discussions including exponential convergence of $\Delta\boldsymbol{\lambda}(t)$ to zero (in a redundant case) or to some constant $\Delta\boldsymbol{\lambda}_\infty$ (in the non-redundant case) as $t \to \infty$ must be omitted in this paper due to the page limitation.

V. Numerical Simulation of 2-D case

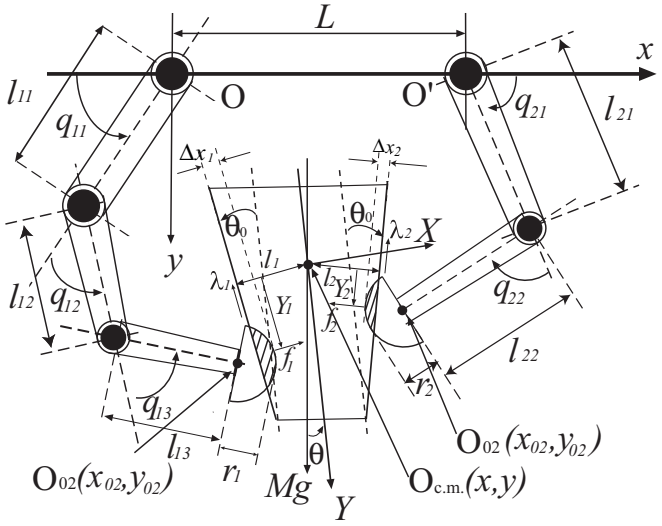

Fig. 3. Two robot fingers pinching an object with non-parallel flat surfaces under the gravity effect

We carried out computer simulation for an object with non-parallel flat surfaces as shown in Fig.3. As in the case of section 2, Lagrange's equation of motion of the overall fingers-object system can be derived if $\boldsymbol{r}_X$ and $\boldsymbol{r}_Y$ are replaced with $\boldsymbol{r}'_{Xi}$ and $\boldsymbol{r}'_{Yi}$ defined as

$$\boldsymbol{r}'_{Xi} = \begin{pmatrix} \cos\left(\theta + (-1)^i\theta_0\right) \\ -\sin\left(\theta + (-1)^i\theta_0\right) \end{pmatrix} \tag{40}$$

$$\boldsymbol{r}'_{Yi} = \begin{pmatrix} \sin\left(\theta + (-1)^i\theta_0\right) \\ \cos\left(\theta + (-1)^i\theta_0\right) \end{pmatrix} \quad i = 1, 2 \tag{41}$$

Then, it is improtant to define the following symbols:

$$\Delta\bar{f}'_i = f_i + (-1)^i\frac{Mg}{2}\sin\left(\theta + (-1)^{-i}\theta_0\right) - \frac{f_d}{r_1 + r_2}\left\{l'_w\cos\theta_0 + (-1)^i d'\sin\theta_0\right\} - \xi_i\left(\Delta x_i\right)\Delta\dot{x}_i \tag{42}$$

$$\Delta\lambda'_i = \lambda_i - \frac{Mg}{2}\cos\left(\theta + (-1)^{-i}\theta_0\right) - \frac{f_d}{r_1 + r_2}\left\{l'_w\sin\theta_0 + (-1)^i d'\cos\theta_0\right\} \tag{43}$$

$$\Delta M = \hat{M} - M,\ \Delta N_i' = \hat{N}_i - (1 - \Delta x_i/r_i)N_i'\ i = 1, 2 \quad (44)$$

where

$$N_i' = -\Big\{ \frac{f_d}{r_1 + r_2} \left(l_w' \sin\theta_0 - (-1)^i d' \cos\theta_0 \right) + \frac{Mg}{2} \cos\left(\theta + (-1)^i \theta_0\right) \Big\} \quad (45)$$

$$d' = (x_{01} - x_{02}) \sin\theta + (y_{01} - y_{02}) \cos\theta \quad (46)$$

$$l_w' = -(x_{01} - x_{02}) \cos\theta + (y_{01} - y_{02}) \sin\theta \quad (47)$$

$$Y_1' - Y_2' = (Y_1 - Y_2) \cos\theta_0 - (l_1 - l_2) \sin\theta_0 \quad (48)$$

$$S' = -f_d \Big\{ l_w' \Big(\frac{r_1 - r_2 - \Delta x_1 + \Delta x_2}{r_1 + r_2} \Big) \sin\theta_0 + d' \Big(1 - \frac{\Delta x_1 + \Delta x_2}{r_1 + r_2} \Big) \cos\theta_0 \Big\} - \frac{Mg}{2} N' \quad (49)$$

$$N' = \sum_{i=1,2} \Big\{ Y_i \sin(\theta + (-1)^i \theta_0) + (-1)^i l_i \cos(\theta + (-1)^i \theta_0) \Big\} \quad (50)$$

In this case, the same form of control signals as that defined in eq.(18) can be applied to dynamics of the overall finger-object system. The closed-loop dynamics is written in the form of (26) to (28) if $\boldsymbol{r}_X$, $\boldsymbol{r}_Y$, $Y_1 - Y_2$, and S are replaced with $\boldsymbol{r}'_{Xi}$, $\boldsymbol{r}'_{Yi}$, $Y_1' - Y_2'$, and S' respectively. In the simulation, the constraints of eqs.(5) and (6) can be ensured by using Baumgarte's method called the CSM (Constraint Stabilization Method). Physical parameters of the fingers-object system are given in Table I and physical gains in control signals are given in Talbe II. Transient responses of principal physical variables appearing in the closed-loop dynamics are shown in Fig.4 from (a) to (j). It is seen from

TABLE I

PHYSICAL PARAMETERS (*in case of 2-D grasp*).

$l_{11} = l_{21}$	length	0.065 (m)
l_{12}	length	0.039 (m)
l_{13}	length	0.026 (m)
l_{22}	length	0.065 (m)
$m_{11} = m_{21}$	weight	0.045 (kg)
m_{12}	weight	0.025 (kg)
m_{13}	weight	0.015 (kg)
m_{22}	weight	0.040 (kg)
$I_{11} = I_{21}$	inertia moment	1.584×10^{-5}(kgm^2)
I_{12}	inertia moment	3.169×10^{-6}(kgm^2)
I_{13}	inertia moment	8.450×10^{-7}(kgm^2)
I_{22}	inertia moment	1.408×10^{-5}(kgm^2)
r_1	radius	0.010 (m)
r_2	radius	0.020 (m)
L base	length	0.063 (m)
M object	weight	0.040 (kg)
l_1	object width	0.013 (m)
l_2	object width	0.023 (m)
h	object height	0.050 (m)
I	inertia moment	1.248×10^{-5}(kgm^2)
θ_0	object inclination angle	-15.00(deg)
k_i(i=1,2)	stiffness	3.000×10^5(N/m^2)
$c_{\Delta 1}$	viscosity	1000(Ns/m^2)
$c_{\Delta 2}$	viscosity	500.0(Ns/m^2)

TABLE II

PARAMETERS OF CONTROL SIGNALS & INITIAL VALUE OF ESTIMATOR

f_d	internal force	1.0 (N)
c_i i=1,2	damping coefficient	0.006 (Nms/rad)
γ_M	regressor gain	0.01
γ_{Ni} i=1,2	regressor gain	0.001
$M(0)$	initial value	0.010(kg)

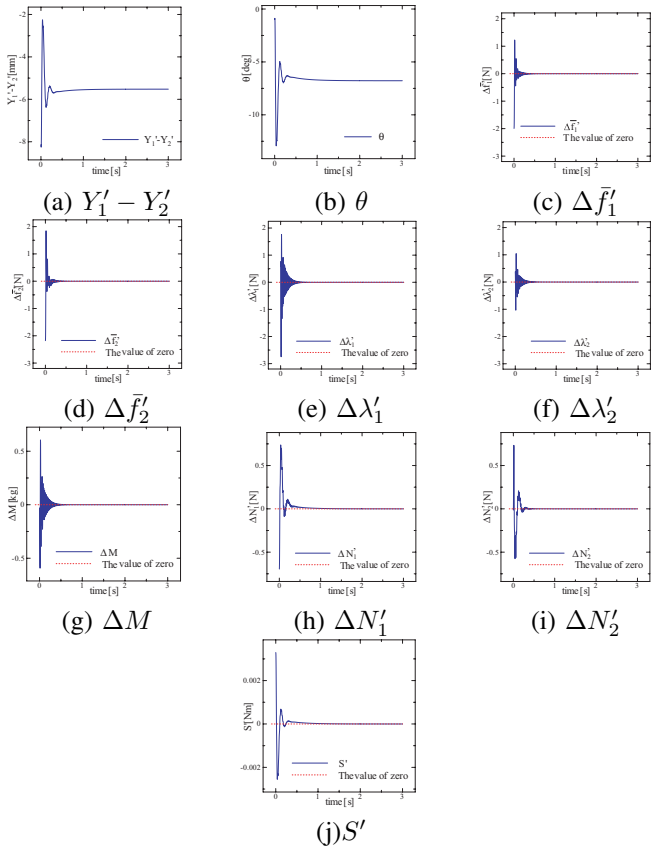

(a) $Y_1' - Y_2'$ (b) θ (c) $\Delta\bar{f}_1'$

(d) $\Delta\bar{f}_2'$ (e) $\Delta\lambda_1'$ (f) $\Delta\lambda_2'$

(g) ΔM (h) $\Delta N_1'$ (i) $\Delta N_2'$

(j)S'

Fig. 4. Transient responses of physical variables

Fig.4 that except $Y_1' - Y_2'$ and θ all magnitudes of constraint forces f_i and $\lambda_i (i = 1, 2)$ converge to their correspponding target values respectively, that is, $\Delta\bar{f}_i'$ and $\Delta\lambda_i'$ converge to zero as $t \to \infty$. Other variables ΔM, $\Delta N_i' (i = 1, 2)$, and S' converge to zero as $t \to \infty$, too. It should be also noted that $Y_1' - Y_2'$ and θ also converge to some constant values as seen from Fig.4 (a) and (b). It should be remarked that in this simulation we intentionally use finger-ends with different sizes ($r_1 \neq r_2$) and an object with non-uniform density (that is, $l_1 \neq l_2$). At the initial position, we set $\Delta x_1 = 0$ and $\Delta x_2 = 0$ and therefore $f_1 = 0$ and $f_2 = 0$. As seen from (c) and (d) of Fig.4, $\Delta\bar{f}_i' (i = 1, 2)$ are around -2.0[N] at $t = 0$ because of $f_1 = f_2 = 0$ at $t = 0$. However, once $f_i > 0$ just after $t > 0$, $f_i(\Delta x_i, \Delta\dot{x}_i) (i = 1, 2)$ are kept to be positive forever, which means that contacts between finger-ends and the object are maintained throughout movements of the overall system.

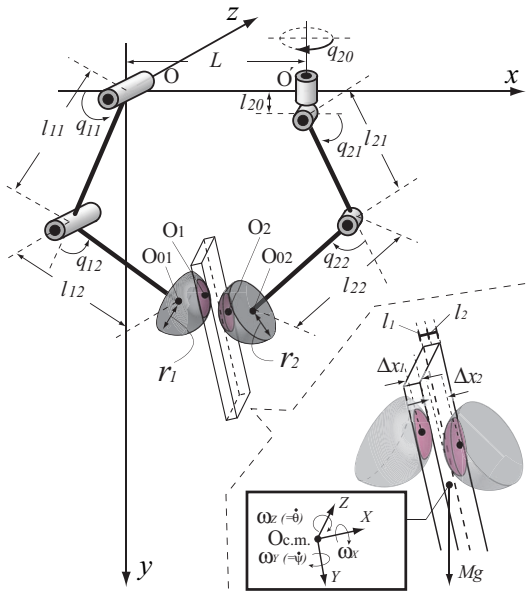

Fig. 5. Two robot fingers pinching a 3-D thin object with parallel flat surfaces under the gravity effect

VI. Numerical Simulation of 3-D case

In this section, previous treatments of 2-D object grasp are extended to 3-D dynamics of pinch motion by a pair of 2-DOF finger (this finger can move only in 2-D space) and 3-DOF finger (that finger can move in 3-D space) as shown in Fig.5. The 3-D overall finger-object system with hemispherical rigid ends has been already analyzed [13]. This 3-D model with rigid finger ends is extended to that of a 3-D model with soft finger ends. The most important difference between rigid finger pinching and soft finger one is that, instead of considering contact constraints between rigid finger ends and a pinched object, soft finger-ends induce a potential energy that can generate reproducing forces and rolling constraints of finger-ends rolling on the object surfaces must be regarded as a movement of the center of contact area without slipping. Another important feature of use of soft fingers is that a stability region for dynamic grasp of a thin object can be enlarged by taking advantage of the visco-elastic property of finger-end material. In order to confirm this, we explore through computer simulations what conditions on control gains are required to realize stable pinching of such thin object by using soft fingers. First, we carried out numerical simulation of pinching motion for a rigid object with width 5.0[mm] and weight 6.667[gram]. In the case of a physical model of dual fingers shown in Fig.5 where the left finger is planar with 2 DOFs and the right finger with 3 DOFs is capable to move in 3-D, it is shown in the previous paper[13] that the principal physical variables converge to some corresponding constant values as $t \to \infty$ as in the following:

$$\begin{cases} \Delta \bar{f}_i \to f_{i\infty},\ \Delta\lambda_{Yi} \to (-1)^{i-1}\lambda_{Y\infty} \\ \Delta\lambda_{Zi} \to (-1)^{i-1}\lambda_{Z\infty},\ \Delta M \to m_\infty,\ \Delta N_i \to n_{i\infty} \\ \Delta N_0 \to n_{0\infty} \end{cases} \quad (51)$$

where the following sensory-motor coordinated control signal is applied:

$$\boldsymbol{u}_i = -c_i\dot{\boldsymbol{q}}_i + (-1)^i \frac{f_d}{r_1+r_2}\boldsymbol{J}_i^{\mathrm{T}}(\boldsymbol{q}_i)(\boldsymbol{x}_{01}-\boldsymbol{x}_{02}) - \frac{\hat{M}g}{2}\left(\frac{\partial y_{0i}}{\partial \boldsymbol{q}_i}\right)^{\mathrm{T}} - r_i\hat{N}_i\boldsymbol{e}_i - r_2\hat{N}_0\boldsymbol{e}_{0i}, \quad i=1,2 \quad (52)$$

where $\boldsymbol{e}_{01} = (0,0)^{\mathrm{T}}$, $\boldsymbol{e}_{02} = (1,0,0)^{\mathrm{T}}$, and $\boldsymbol{e}_1 = (1,1)^{\mathrm{T}}$, $\boldsymbol{e}_2 = (0,1,1)^{\mathrm{T}}$. $\hat{M}$, $\hat{N}_i (i=1,2)$, and $\hat{N}_0$ are estimated values as in the following:

$$\hat{M}(t) = \hat{M}(0) + \int_0^t \frac{g\gamma_M^{-1}}{2}\sum_{i=1,2}\left(\frac{\partial y_{0i}}{\partial \boldsymbol{q}_i}\right)^{\mathrm{T}}\dot{\boldsymbol{q}}_i\,\mathrm{d}\tau \quad (53)$$

$$\hat{N}_i(t) = \hat{N}_i(0) + \int_0^t \gamma_{Ni}^{-1} r_i \boldsymbol{e}_i^{\mathrm{T}}\dot{\boldsymbol{q}}_i(\tau)\mathrm{d}\tau \quad (54)$$

$$= \hat{N}_i(0) + \gamma_{Ni}^{-1} r_i \boldsymbol{e}_i^{\mathrm{T}}\left(\boldsymbol{q}_i(t) - \boldsymbol{q}_i(0)\right) \quad (55)$$

$$\hat{N}_0(t) = \hat{N}_{N0}(0) + \frac{r_2}{\gamma_0}q_{20}(t) \quad (56)$$

Note that $\hat{N}_0$ appears in the control input for 3-D motion of the right finger so that q_{20} induces rotation around the y axis. Table III shows numerical data of physical parameters of the robot fingers and pinched object. Parameters of control signals and initial values of estimators $\hat{M}$ and $\hat{N}_i$ are given in Table IV. From transient responses in Fig.6, $\Delta\bar{f}_i$, $\Delta\lambda_{Yi}$, and $\Delta\lambda_{Zi}$ converge to f_∞, $(-1)^{i-1}\lambda_{Y\infty}$, and $(-1)^{i-1}\lambda_{Z\infty}$ as $t \to \infty$ respectively. Similarly, $\Delta N_i (i=1,2)$ and ΔN_0 converge to $n_{i\infty}$(i=1,2) and $n_{0\infty}$ as $t \to \infty$ respectively

TABLE III

Physical Paramaters (*in case of 3-D grasp*)

l_{11}=l_{21}	length	0.040 (m)
l_{12}=l_{22}	length	0.040 (m)
l_{20}	length	0.000 (m)
$m_{11} = m_{21}$	weight	0.045 (kg)
$m_{12} = m_{22}$	weight	0.035 (kg)
m_{13}	weight	0.020 (kg)
$I_{xx11} = I_{xx21}$	inertia moment	5.625×10^{-7}(kgm^2)
$I_{yy11} = I_{yy21}$	inertia moment	1.613×10^{-5}(kgm^2)
$I_{zz11} = I_{zz21}$	inertia moment	1.613×10^{-5}(kgm^2)
$I_{xx12} = I_{xx21}$	inertia moment	4.375×10^{-7}(kgm^2)
$I_{yy12} = I_{yy21}$	inertia moment	1.254×10^{-5}(kgm^2)
$I_{yy22} = I_{yy22}$	inertia moment	1.254×10^{-5}(kgm^2)
r_0	link radius	0.005 (m)
r_i(i=1,2)	radius	0.01 (m)
L	base length	0.063 (m)
M	object weight	6.667×10^{-3} (kg)
l_i(i=1,2)	object width	2.500×10^{-3} (m)
h	object height	0.050 (m)
k_i (i=1,2)	stiffness	3.000×10^5(N/m^2)
$c_{\Delta i}$(i=1,2)	viscosity	1000(Ns/m^2)

TABLE IV

Parameters of Control Signals and Initial values

f_d	0.100 (N)	c_i (i=1,2)	0.006
c_{q20}	0.006	γ_M	0.001
γ_{Ni}(i=1,2)	0.001	γ_{N0}	0.001
$M(0)$	0.000 (kg)	$\hat{N}_1(0)$	0.000 (N)
$\hat{N}_2(0)$	0.000 (N)	$\hat{N}_0(0)$	0.000 (N)

according to Fig.6. S_Y and S_Z also converge to some constant values as $t \rightarrow \infty$ respectively, which show that the rotational moments affecting the pinched object converge to zero (the torque balance is achieved). Therefore, these variables eventually tend to satisfy eq.(51) that corresponds to a certain equilibrium state. It is confirmed that stable grasping in 3-D space was realized in a dynamic sense by a pair of robot fingers with hemispherical and soft tips.

Next, we tried to examine the case of a thinner and light object with width 1.0[mm] and weight 1.333[gram] like a credit card. When we used the same values for viscosity $c_{\Delta i}$, stiffness k_i, and damping constants c_i as in Table III and ran the simulation based on the same control gains as in Table IV, the trajectories of state variables did not converge in the sequel. The material of finger-tips should be a little softened. Hence, we changed physical parameters of the finger-tip material to those in Table V and decreased the value of f_d to the level of $f_d = 0.010$[N] as given in Table VI. Then, we could obtain a successful result as shown in Fig.7. As seen in Fig.7 all principal physical variables tend to their corresponding constant values as $t \rightarrow \infty$, which shows

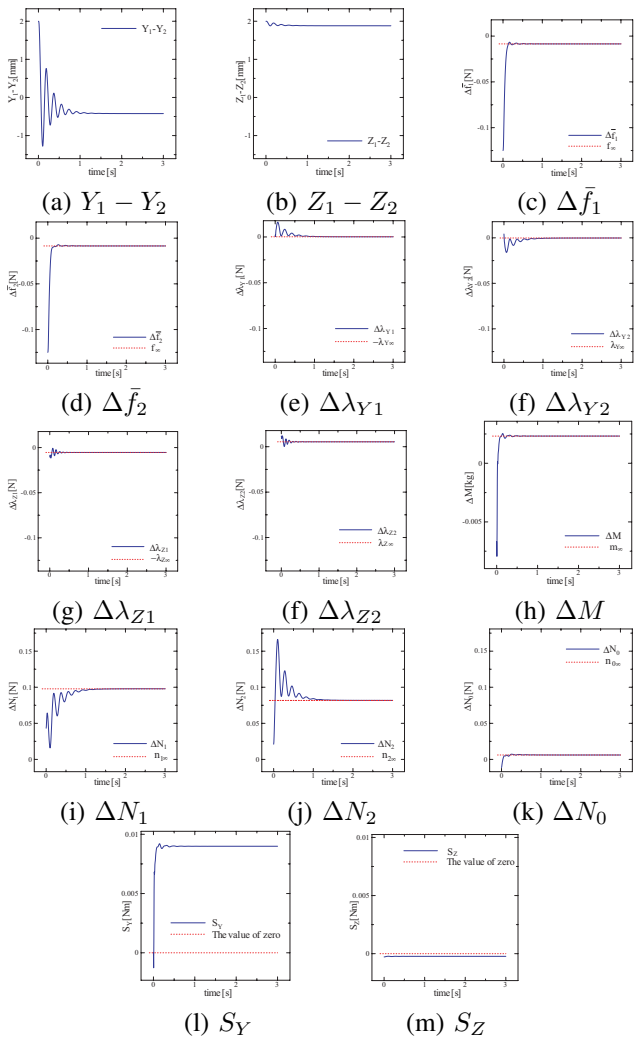

Fig. 6. Transient responses of physical variables

TABLE V

PHYSICAL PARAMATERS

M	object weight	1.333×10^{-3} (kg)
l_i(i=1,2)	object width	0.500×10^{-3} (m)
h	object height	0.050 (m)
k_i	stiffness parameter	1.000×10^5(N/m^2)
$c_{\Delta i}$(i=1,2)	viscosity parameter	300.0(Ns/m^2)

TABLE VI

PARAMETERS OF CONTROL SIGNALS AND INITIAL VALUES

f_d	0.010 (N)	c_i (i=1,2)	0.006
c_{q20}	0.006	γ_M	0.001
γ_{Ni}(i=1,2)	0.001	γ_{N0}	0.001
$M(0)$	0.000 (kg)	$\hat{N}_1(0)$	0.000 (N)
$\hat{N}_2(0)$	0.000 (N)	$\hat{N}_0(0)$	0.000 (N)

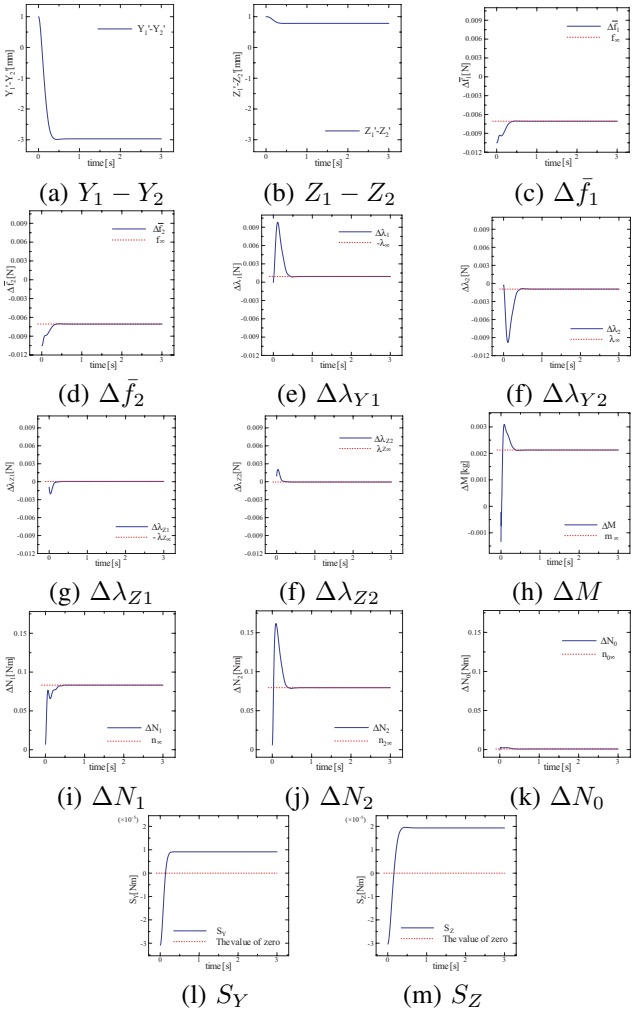

Fig. 7. Transient responses of physical variables

accomplishment of stable blind grasping in a dynamic way.

VII. CONCLUSIONS

This paper shows that there exists a class of control signals constructed from using only finger kinematics and measurement data of finger joint angles that enable a pair of multi-d.o.f fingers with soft finger-tips to grasp a rigid object

securely and manipulate it towards an equilibrium state of force/torque balance. This shows that even a pair of robot fingers can grasp an object securely in a blind manner like human grasp it even if their eyes are closed. A sketchy proof of convergence of solution trajectories of the closed-loop dynamics toward an equilibrium state satisfying force/torque balance is given in a 2-D case. From computer simulations, it is shown that physical parameters of stiffness and viscosity of the finger-end soft material are sensitive to performances of stable motion of grasping. It is also shown from simulations that gain-tunings of control parameters based upon rough prediction of the object width and weight must be important, since "blind grasping" is feasible once adequate control gains are chosen and fixed.

Experimental results on blind grasping by using a pair of soft robot fingers are omitted in this paper due to page limitation but will be shown in a movie accompanied with this paper submissionw.

REFERENCES

[1] M. R.Cutkovsky, *Robotic Grasping and Fine Manipulation*, Kluwer Academic, Dordrecht, Netherlands; 1985.

[2] K. B. Shimoga, "Robot grasp synthesis algorithms: A survey", *Int. J. of Robotics Research*, vol.15, no.3, 1996, pp.230-266.

[3] J. D. Crisman, C. Kanojia, and I. Zeid, "Graspar: A flexible, easily controllable robotic hand", *IEEE Robotics and Automation Magazine*, June, 1996, pp.32-38.

[4] A. M. Okamura, N. Smaby, and M. R. Cutkovsky, "An overview of dexterous manipulation", *Proc. of the 2000 IEEE Robotics and Automation*, SanFrancisco, CA, April, 2000, pp.255-262.

[5] R. M. Murray, Z. Li, and S. S. Sastry, *A Mathematical Introduction to Robotic Manipulation*, CRC Press, Boca Raton and Tokyo; 1994.

[6] John Napier, *Hands*, Princeton Univ. Press, Princeton, NJ, 1993.

[7] D.J. Montana, "Contact stability for two-fingered grasps", *IEEE Trans. on Robotics and Automation*, vol.8, no.4, 1992, pp.421-430.

[8] S. Arimoto, P.T.A. Nguyen, H.-Y. Han, and Z. Doulgeri, "Dynamics and control of a set of dual fingers with soft tips", *Robotica*, vol.18, no.1, 2000, pp.71-80.

[9] Z. Doulgeri, J. Fasoulas, and S. Arimoto, "Feedback control for object manipulation by a pair of soft tip fingers", *Robotica*, vol.20, No.1, 2002, pp.1-11.

[10] S. Arimoto, M. Yoshida, J.-H. Bae, and K. Tahara, "Dynamic force/torque balance of 2D polygonal objects by a pair of rolling contacts and sensory-motor coordination", *Journal of Robotic Systems*, vol.20, no.9, 2003, pp.517-537.

[11] S. Arimoto, "Intelligent control of multi-fingered hands", *Annual Review in Control*, vol.28, no.1, 2004, pp.75-85.

[12] S. Arimoto, R. Ozawa, and M. Yoshida, "Two-dimensional stable blind grasping under the gravity effect", *Proc. of the 2005 IEEE Int. Conf. on Robotics and Automation*, Barcelona, Spain, 2005, pp.1208-1214.

[13] S. Arimoto, M. Yoshida, and J.-H. Bae, "Stability of 3D-Object Grasping under Non-Holonomic Constraints and the Gravity Effect",*8th Int. IFAC Symposium on Robot Control*, Bologna, Italy, 2006, R-046.

[14] S. Arimoto, *Control Theory of Nonlinear Mechanical Systems: A Passivity-based and Circuit-theoretic Approach*, Oxford University Press, Oxford; 1996.